J Nanostruct 16(4): 5613-5621, Autumn 2026

RESEARCH PAPER

Laser Ablation Assisted Preparation and Photo Catalytic of Au/ZnO Nano Solution

*Nadia Mohammed Jassim *, Hanan Khalid Owda, Nada Abdul Hadi Kareem*

College of Science, Diyala University, Diyala 4200, Iraq

ARTICLE INFO

Article History:
Received 03 June 2026
Accepted 27 August 2026
Published 01 October 2026

Keywords:
Au-ZnO-NPs
Gold nanoparticles
Laser ablation
Methylene blue
Zinc oxide nanoparticles

ABSTRACT

In this work, the photo catalytic efficiency of nanoparticles (gold, zinc oxide nanoparticles, and gold-zinc oxide) and their effect on the degradation of methylene blue (MB) dye were studied. The deionized water extraction method was used to prepare these nanoparticles, and the prepared samples were characterized using several techniques, such as XRD, UV-Vis spectroscopy, FTIR spectroscopy, and TEM, FESEM. The results demonstrated the successful synthesis of nanoparticles with high crystallinity and small nanoscale size. Gold and zinc nanoparticles exhibited a significant red-shift in UV-vis absorption and improved charge separation, resulting in enhanced photo catalytic activity under UV-A light. This study confirmed that gold-zinc oxide nanoparticles were highly efficient in degrading methylene blue (MB) dye, thanks to the synergistic effect between gold and zinc oxide, which reduced the band gap and improved light absorption. These results indicate that gold and zinc nanoparticles have promising potential as effective photo catalysts in wastewater treatment applications.

How to cite this article
Jassim N., Owda H., Kareem N. Laser Ablation Assisted Preparation and Photo Catalytic of Au/ZnO Nano Solution. J Nanostruct, 2026; 16(4):5613-5621. DOI: 10.22052/JNS.2026.04.091

INTRODUCTION

Nanoparticles synthesized by laser ablation methods are widely used in nonlinear optics [1]. With this technology, much larger and different materials are minuscule reduced to atomic size, yielding nanoparticles. Particles in the dimension range of (1 to 100 nanometer) sized nanoparticles or NPs. These NPs are really special because small size, very high carrier capacity, significant surface area per volume ratio, great reactiveness and easy to modification of surface properties [2].

Because of the coherence property of laser beam it has been possible to examine the behavior of light in optical materials at high intensities higher than those found in conventional light sources. Therefore, the laser has a high intensity that enables it to modify the optical properties of materials.

Nanomaterials have also received great attention due to their application in various fields such as medicine, environment, energy and communications, so the NLO properties of nanomaterial composite have received attention due to their applications in optical switching and photovoltaic devices [3–6].

Photocatalyst is a branch of chemistry which

* *Corresponding Author Email: nadiajassim@uodiyala.edu.iq*

This work is licensed under the Creative Commons Attribution 4.0 International License.
To view a copy of this license, visit http://creativecommons.org/licenses/by/4.0/.

used light and a photocatalyst to stimulate the chemical reactions [5]. Photocatalysis is a Greek-derived term consisting of photo meaning light and articulating words into "catalysis", which comes from the verb katergatzai, meaning "to dissolve". It means that a reaction must occur in the presence of a semiconductor illuminated by light [7–10].

Among all these metal oxides, zinc oxide nanoparticles (ZnO) have received widespread attention due to their catalytic properties, such as a high band gap (3.37 eV) at room temperature and a large exciton bindin energy (60 MeV), their optical properties, high catalytic activity, anti-inflammatory and wound-healing properties, and UV filtering. They have also been used as biosensors for cholesterol, enzyme biochemistry, and biosensing [6,8].

In addition to the above advantages of zinc oxide catalysts, they are also low cost, photoactive and widely available. The wide band gap of zinc oxide is a major drawback that makes it less efficient for solar applications, but promising for UV detection. However, nanostructures composed of noble metals and zinc oxide can overcome this dilemma. To support visible light detection, metal nanoparticles will absorb visible light and will generate localized plasmonic resonances. Therefore, the noble metal gold nanoparticles with wide band gap semiconductor zinc oxide is among the most convenient approaches toward enhancing UV-visible photodetection [7,11].

Due to the exceptional ability of gold nanoparticles to strongly absorb electromagnetic waves at the surface plasmon resonance in the visible range and the ability to remain evenly distributed in the presence of a matrix, they have attracted widespread interest and use in various fields, such as sensors, electronic devices, medical treatments, catalysts, solar cells, and drug delivery [12,13].

Laser ablation in liquid (LAL) is the technique for producing nanostructures by ejecting material through laser pulse irradiation onto a solid target, which is placed in liquid. Laser-matter interaction and further ablation highly depend on the pulse energy and its duration, kind of background liquid, geometry and morphology of samples, as well as focusing condition [14].

The use of ablation by pulsed laser in liquids for nanomaterials fabrication is become a chemically very simple and clean technique, presenting the opportunity to have high of purity products(15).

MATERIALS AND METHODS

Samples preparation

A gold pellet is placed in a beaker, and 10 ml of deionized water is added. It is irradiated with an neodymium:YAG laser at a wavelength of 1064 nm, a frequency of 1 Hz, and a pulse duration of 9 ns. The ablation process is performed for 500 pulses, involving 500 mJ of laser energy focused onto the target. Zinc oxide nanoparticles (NPs) are prepared using the same laser parameters, except that the laser energy is set to 700 mJ, and the pulse number is increased to 750 mJ. Bulk zinc oxide is immersed in deionized water in the same manner. To prepare core-shell (Au-ZnO) nanoparticles, the zinc target is immersed in the previously prepared Au NP solution. The same laser is used, but with an energy of 700 mJ and a pulse duration of 500 ns. Fig. 1 illustrates the practical steps for preparing the nanomaterials. After preparation, the gold nanoparticle solution appears bright red, while the zinc oxide nanoparticle solution is light gray as shown in Fig. 2.

Method

The research investigated how ZnO, Au, and ZnO/Au nanoparticles (NPs) effect the photodegradation of MB dye exposed to sunlight, to establish a pollution model. The wavelength of 664 nm was chosen as that characteristic of the MB dye, which will would be analyzed to determine the photodegradation of this industrial pollutant. Briefly:

1- A 2mg/L of MB dye solution was prepared and stirred thoroughly for three hours.

2- A thin layer of NPs (25 mL of solution) was then coated on a glass substrate at low temperature and mixed with (50 mL) of the MB dye solution.

3- The sample was placed in dark for approximately 30 minutes to ensure that the (MB dye) maintained an equilibrium between adsorption and desorption on the photocatalyst's surface.

4- To measure the change in absorbance, UV-Vis spectroscopy was used by taking 3 ml of the solution every 30 minutes, and the absorbance of the solutions was measured at intervals ranging from 30 to 180 minutes.

5- The results showed that the time length of exposure increases, the absorbance decreases,

CC BY

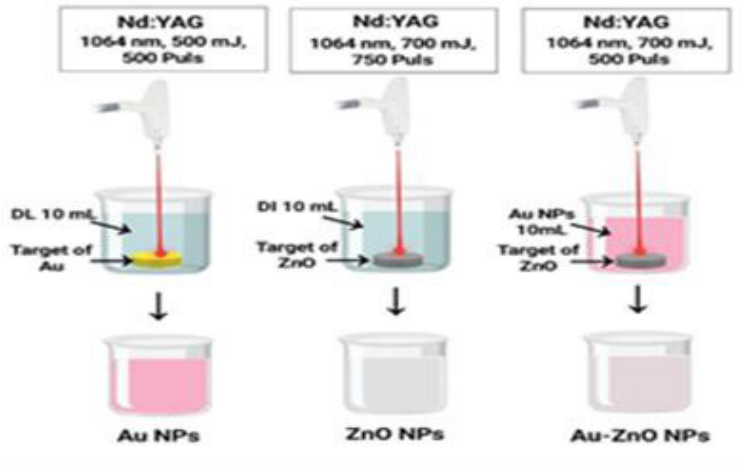

Fig. 1. Steps of preparation

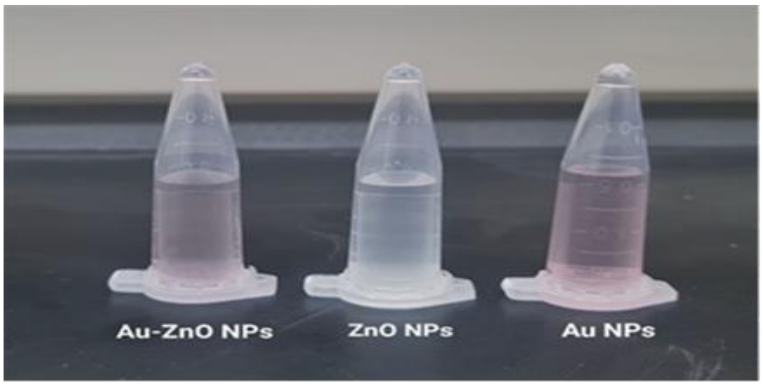

Fig. 2. Shown samples color of nanoparticles after laser preparation.

Table 1. Shows the Crystallite size (D) of Au NPs and ZnO NPs that measured from Scherrer's equation:

NPs	2theta (degree)	hkl	FWHM (deg)	2 theta (Rad.)	FWHM (Rad)	D (nm)	Average crystallite size (nm)
ZnO	31.71508	104	0.140568	0.277	0.002	58.729	27.289
	36.06389	110	0.94464	0.315	0.016	8.841	
	56.2419	110	0.62976	0.491	0.011	14.298	
Au	38.11825	110	0.15744	0.333	0.003	53.365	30.727
	44.36457	110	0.31488	0.387	0.005	27.236	
	64.59441	110	0.94464	0.564	0.016	9.945	
	77.61192	110	0.31488	0.677	0.005	32.363	

(cc) BY

Among all samples, the gold and zinc nanoparticles showed the highest photocatalytic efficiency, outperforming the gold and zinc nanoparticles alone.

The photodegradation efficiency of this MB dye can calculated by using the Eq. 1:

Degradation efficiency % = [1- C_t/C_0] × 100

(C_0) is the absorbance before exposure,
(C_t) is the absorbance of the MB dye after exposure to sunlight.

RESULTS AND DISCUSSION

The X-ray diffraction pattern of the nanoparticles shown in Fig. 3. The Fig. 3A shows three significant peaks are thus revealed. Peaks corresponding to 2θ = 44.1° are attributed to (200), while peaks at 64.5° are assigned to (220) and peaks at 77.6° to (311); thus proving the cubic face-centered structure of gold by the (JCPDS) card No. 00-004-0784. The peaks' clarity, sharpness, and greater intensity indicate the high crystallinity and good purity of the synthesized particles. Fig. 3B shows the XRD analysis of ZnO NPs, the diffractograms show peaks that correspond to three specific angles at 2θ = 31.7°, 36.0°, and 56.2Which relate to levels (100), (101), and (110) respectively, which confirms that the manufactured particles have a hexagonal structure of the wurtzite type, and this is consistent with reference card No. 01-079-0207. The broadness of the peaks shows also a small crystal size that corroborates that the particles were formed in nanoscale dimensions. Fig. 3C. The peak at 36.2° corresponds to the (101) crystal plane of the hexagonal ZnO structure of wurtzite, indicating that the ZnO particles have good crystallinity. Due to the very small nanoscale size of Au particles or their highly distributed nature over the surface of ZnO, the presence of clear peaks for gold is missing, thereby disturbing the clarity of the crystalline reflections in the XRD pattern. The Scherrer Eq. 2 is used to calculate the crystal size of the gold and zinc nanoparticles, as shown in Table 1.

$$D = \frac{K\lambda}{\beta \cos\theta} \quad (1)$$

Where, D: the particle size, K: is Scherrer's constant = 0.9, β: full width of half maximum (FWHM) in radians.

Fig. 4. UV-Visible absorbtion spectra of (A) gold nanoparticles, (b) zinc oxide nanoparticles, (c) gold-zinc oxide nanoparticles. Fig. 4 shows that the peak at 525 nm for Au NPs is the strongest peak, located in the visible range, due to surface

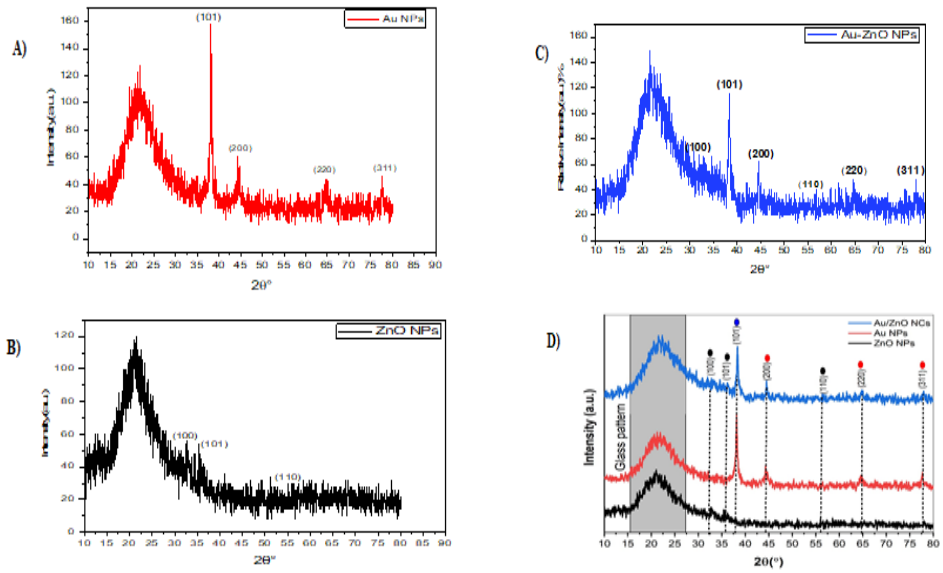

Fig. 3. X-ray diffraction analysis spectra of (A) gold nanoparticles, (B) zinc oxide nanoparticles,(C) Au-ZnO nanoparticles , (D) standard reference patterns (JCPDS) no. 400-004-0784 and no. 01-079-0207 .

CC BY

plasmonic resonance. Fig. 4B shows that the absorption peak of ZnO is strong in the wavelength (342) nm. Fig. 4C we notice that the peak intensity of the absorption of zinc nanoparticles has shifted from (342) nm to (345)nm, while the second peak (529) nm is the gold nanoparticles due to the local surface plasmon resonance (LSPR) which absorbs light in the visible light range.

Fig. 5 illustrates the Fourier Transform Infrared Spectroscopy of Au NPs, ZnO NPs, Au-ZnO NPs. Fig. 5A shows that the peak at 3275 cm^{-1} indicating O–H stretching vibration. The band at 1637 cm^{-1} corresponding to C=O or O-H group. The band at 2163 cm^{-1} indicating C≡C (alkynes) or C≡N (nitriles) triple bonds. Fig. 5B shows that the peak at 3269 cm^{-1} indicating stretching vibrations of the O-H bond. The band at 1636 cm^{-1} corresponding to O-H bond in water molecules adsorbed on the ZnO surface. The band at 2135 cm^{-1} is triple bond vibrations such as C≡C (alkynes) or C≡N (nitriles). Fig. 5C shows that the peak at 3269 cm^{-1} was stretching vibrations of the O-H bond. The band at 2169 cm^{-1} indicating C≡C (alkynes) or C≡N (nitriles). The peak at 1637 cm^{-1} is attributed to the bending vibration of (O-H) bonds or (C=O) bonds.

Fig. 6. Shown the FESEM pictures for (A) gold NPs, (B) zinc oxide NPs, (C) gold-zinc oxide NPs. Fig. 6A shown the surface morphology of the Au NPs with magnifications 50.00 KX and 20.00 KX and a scale bar of 200 nm. The results indicate that the nanoparticles exhibit an aggregate-like structure, forming compact clumps. The particle size distribution ranges from 18.63 nm to 28.12 nm, indicating agglomeration. Fig. 6B illustrate the surface morphology of ZnO nanoparticles with 50.00 KX and 20.00 KX magnifications and a scale bar of 200 nm. The results show that ZnO NPs are exhibit irregular and clustered in shape with particle size distribution ranging from (27.95-49.68) nm. Fig. 6 The particles appear in approximately spherical or irregular shapes within the nano range, and can be uniformly distributed or stacked depending on the preparation conditions. The presence of Au NPs improved the optical and electrical properties of zinc oxide, and they usually appear as brighter spots on the surface.

Fig.7 Display the transmission electron microscopy (TEM) pictures for (A) gold

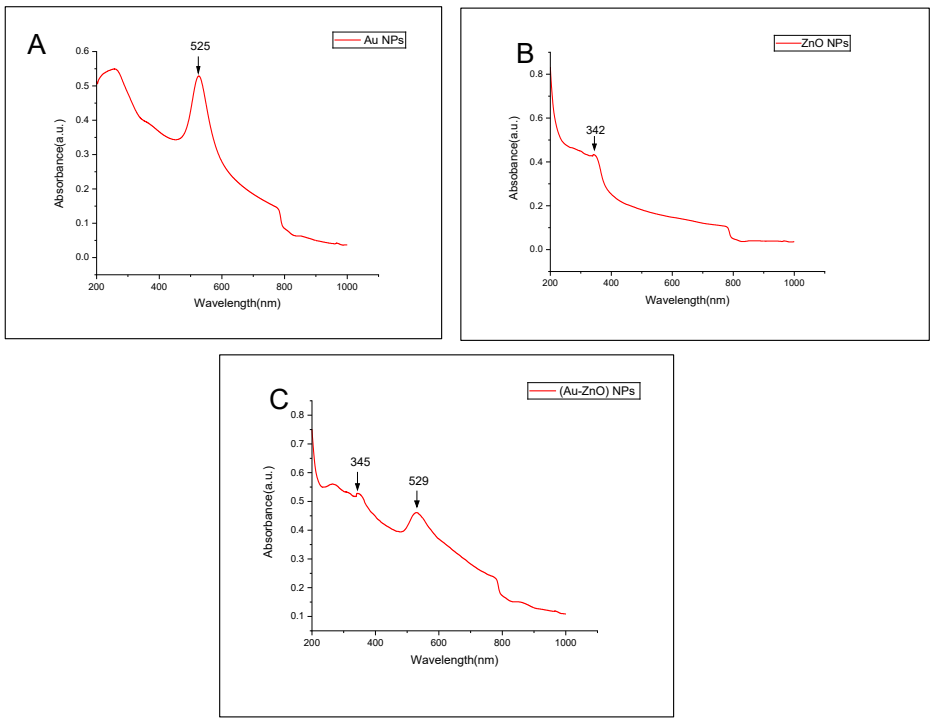

Fig. 4. The UV-Vis pattern of)A) gold nanoparticles,)B) zinc oxide nanoparticles,)C) gold-zinc oxide nanoparticles.

nanoparticles, (B) zinc oxide nanoparticles, (C) gold-zinc oxide nanoparticles. Fig. 7A shows Au nanoparticles with 100.000 KX magnifications and scale image of 30 nm the Au NP. The TEM picture showed that majority of Au NPs have a dark gray or black color. Also it have spherical or nearly spherical shape with some agglomeration. Fig. 7B shows ZnO nanoparticles with 45.460 KX magnifications and scale image of 80 nm the ZnO NPs. The TEM image demonstrated that the ZnO nanoparticles appears dark gray. Fig. 7C shows Au-ZnO nanoparticles with 100.000 KX magnifications and scale image of 30 nm, the gold nanoparticles are surrounded by zinc oxide. The black spheres in the figure are gold nanoparticles surrounded by zinc oxide, and have some clumping.

Fig. 8 shows the photocatalysis activity response of)A) gold NPs,)B)zinc oxide NPs,)C) gold-zinc oxide NPs, and (d) efficiency of NPs. Fig. 8A It shows that the experiment was conducted in the dark, so no photocatalytic activity occurred, and the absorbance remained high, indicating that no dye degradation had occurred. In the experiments from Au 30 min to Au 180 min, the absorbance decreased with increasing light exposure, indicating degradation of the MB dye. This indicates that the gold nanoparticles have a catalytic effect that efficiently degrades the dye under the influence of light, with the degradation efficiency increasing over several hours of exposure. Fig. 8B shows that the experiment was conducted in the dark, meaning that light was not present, and therefore no photocatalytic activity could occur. The absorbance remained high because the dye degradation did not occur. In the experiments from ZnO 30 min to ZnO 180 min, as the exposure time increased, the absorbance decreased, indicating degradation of the MB dye. This confirms that ZnO nanoparticles effectively catalyze the degradation of the dye under the influence of light, and the degradation efficiency increases with increasing exposure time. Fig. 8C illustrates the effect of photo catalytic activity of Au-ZnO NPs on the degradation of the material through changes in absorbance.

The results confirmed that the gold - zinc

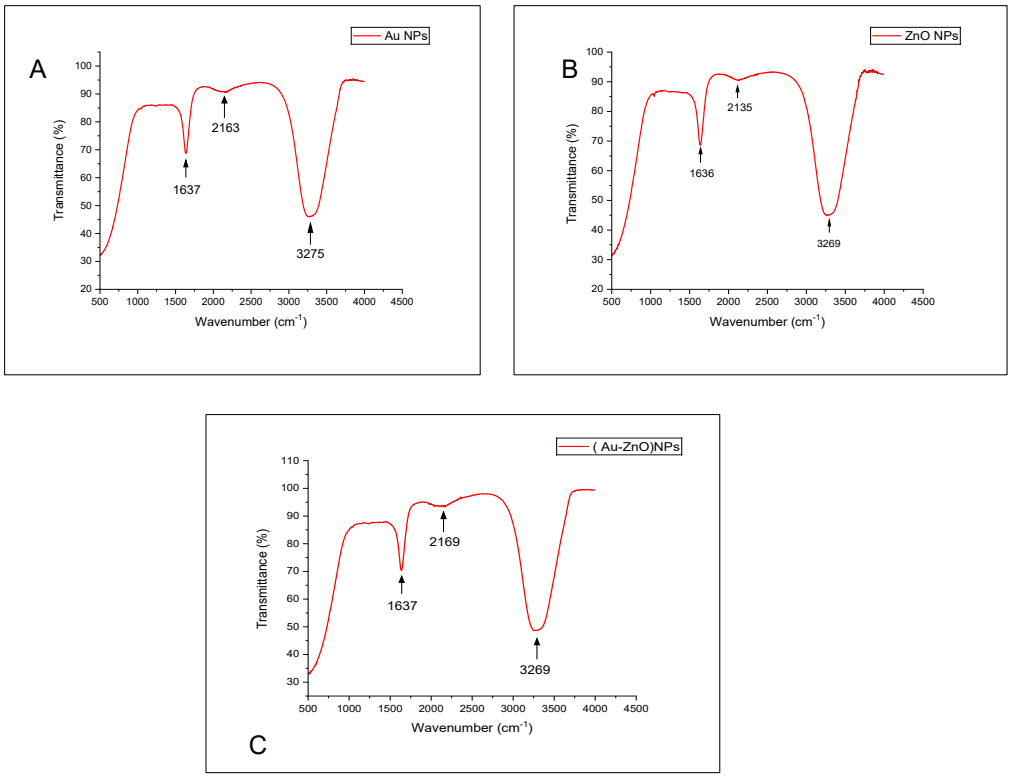

Fig. 5. Shown Fourier Transform Infrared Spectroscopy spectrum of)A) gold nanoparticles)B) zinc oxide nanoparticles and)C) gold-zinc oxide nanoparticles.

CC BY

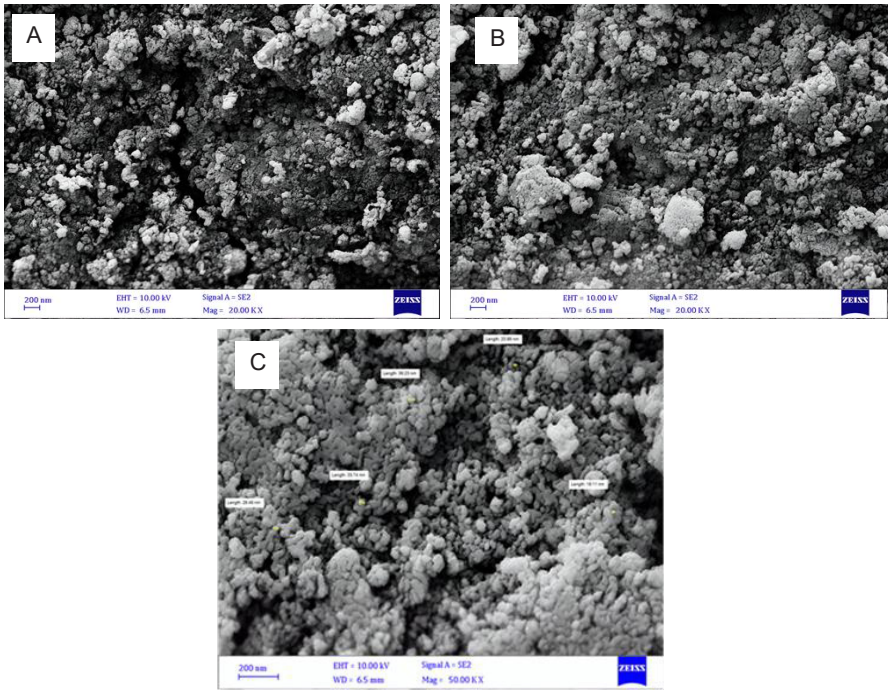

Fig. 6. Shown the Field Emission Scanning Electron Microscopy (FESEM) pictures for (A) gold NPs,)B) zinc oxide NPs,)C) gold-zinc oxide NPs.

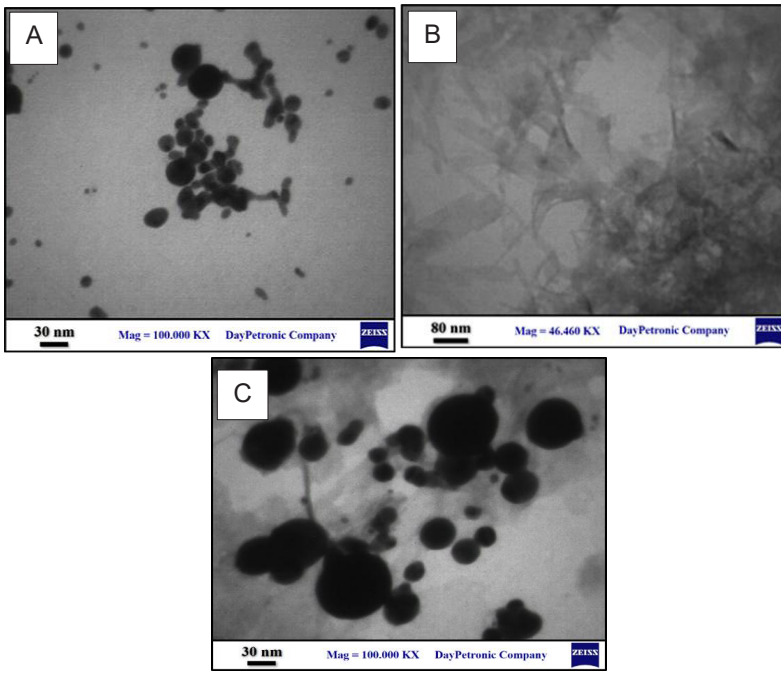

Fig. 7. Image of the Transmission Electron Microscopy (TEM) of)A) gold NPs ,)B) zinc oxide NPs,)C) gold-zinc oxide NPs.

CC BY

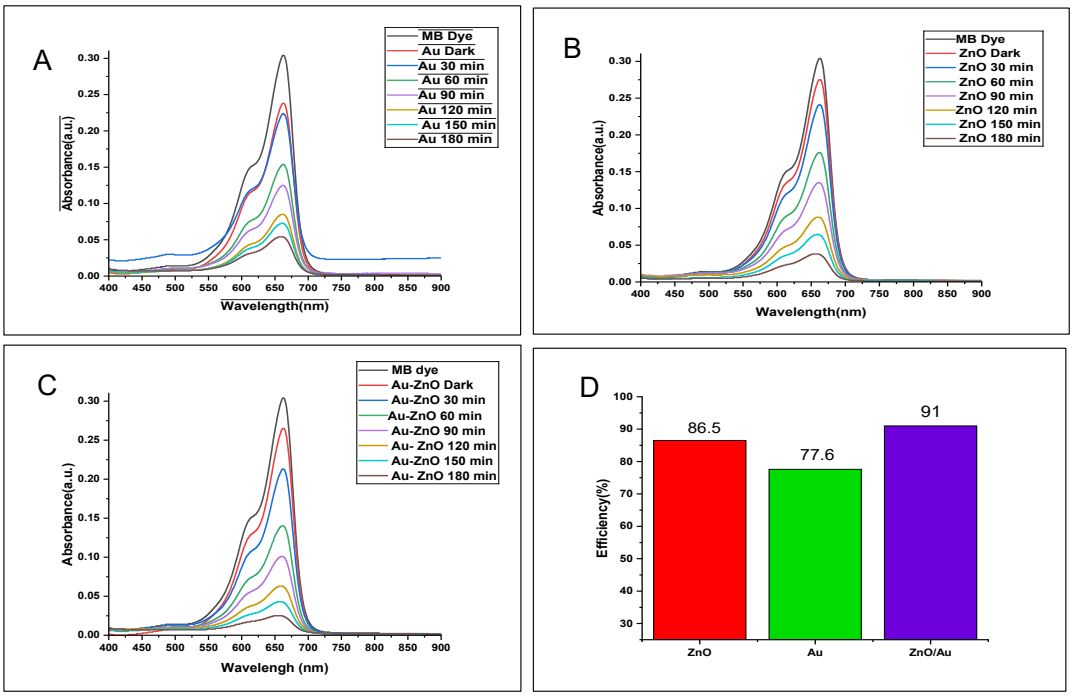

Fig. 8. Show the photocatalysis activity for (A) gold NPs,)B) zinc oxide NPs,)C) gold-zinc oxide NPs, (D) Efficiency of nanoparticles.

oxide nanoparticles possess highly efficient photocatalytic activity, compared to the photocatalytic efficiencies of Au NPs and ZnO NPs alone. Fig. 8D shows that the Au-ZnO composite is the most efficient in the degradation of dyes, thus proving the enhanced photoactivity caused by the synergistic interaction of gold with zinc oxide nanoparticles.

CONCLUSION

The experimental results showed that the pulsed laser ablation method for producing Au nanoparticles, ZnO nanoparticles, and Au-ZnO nanoparticles was a successful method.

Structural and spectroscopic analyses revealed that doping zinc oxide with gold significantly improves its optical and photocatalytic properties by enhancing light absorption and separating electrons from holes. The Au–ZnO system showed superior performance in degrading methylene blue under UV-A irradiation compared to pure AuNPs and ZnO-NPs. This enhancement results from the combined interaction of Au and ZnO, which facilitates charge transfer and extends the photocatalytic response to the visible spectrum. Therefore, Au–ZnO nanoparticles are future candidates for the development of efficient and environmentally friendly photocatalysts for water purification.

CONFLICT OF INTEREST

The authors declare that there is no conflict of interests regarding the publication of this manuscript.

REFERENCES

1. Chen L, Hong M. Functional nonlinear optical nanoparticles synthesized by laser ablation. Opto-Electronic Science. 2022;1(5):210007.
2. Kamil AA, Bakr NA, Mubarak TH, Al-Zanganawee J. Synthesis and study of the optical and structural properties of Au and Ag nanoparticles by pulsed laser ablation (PLAL) technique. Digest Journal of Nanomaterials and Biostructures. 2021;16(4):1219-1226.
3. Jassim NM, Ibrahim NI. Z-Scan Study of the Non-linear Optical Properties of Silver/Curcumin Dye Nanocomposites Prepared Via Nanosecond Pulsed Laser Ablation. Revue des composites et des matériaux avancés. 2024;34(4):533-540.
4. Al-Asady Z, Al-Hamdani A. Diffraction Rings Pattern and Nonlinear Optical Properties of Hybrid ZnO-NPs / Epoxy Resin. Engineering and Technology Journal. 2020;38(3A):440-445.
5. Ameta R, Solanki MS, Benjamin S, Ameta SC. Photocatalysis.

CC BY

Advanced Oxidation Processes for Waste Water Treatment: Elsevier; 2018. p. 135-175. http://dx.doi.org/10.1016/b978-0-12-810499-6.00006-1
6. Jassim NM. Synthesis and nonlinear optical responses of Ag: ZnO core: shell nanoparticles induced by Z-scan technique. Journal of Optics. 2024;55(4):3283-3292.
7. Jassim NM, Wang K, Han X, Long H, Wang B, Lu P. Plasmon assisted enhanced second-harmonic generation in single hybrid Au/ZnS nanowires. Opt Mater. 2017;64:257-261.
8. Kalpana VN, Devi Rajeswari V. A Review on Green Synthesis, Biomedical Applications, and Toxicity Studies of ZnO NPs. Bioinorg Chem Appl. 2018;2018:1-12.
9. H. Mubarak T, M. Jassim N, A. Guidan Q. Some physical properties of Al nanoparticle Via pulse laser ablation in liquid method (PLAl). Academic Science Journal. 2023:65-81.
10. Mohamadpour F, Amani AM. Photocatalytic systems: reactions, mechanism, and applications. RSC Advances. 2024;14(29):20609-20645.
11. Spitaleri L, Nicotra G, Zimbone M, Contino A, Maccarrone G, Alberti A, et al. Fast and Efficient Sun Light Photocatalytic Activity of Au_ZnO Core–Shell Nanoparticles Prepared by a One-Pot Synthesis. ACS Omega. 2019;4(12):15061-15066.
12. Hettiarachchi BS, Takaoka Y, Uetake Y, Yakiyama Y, Yoshikawa HY, Maruyama M, et al. Mechanistic Study in Gold Nanoparticle Synthesis through Microchip Laser Ablation in Organic Solvents. Metals. 2024;14(2):155.
13. Plasmonic Enhancement in Molecular Fluorescence of Natural Curcumin Dye with Silver Nanoparticles Synthesis and Biological Application. Journal of Pharmaceutical Negative Results. 2022;13(3).
14. Fazio E, Gökce B, De Giacomo A, Meneghetti M, Compagnini G, Tommasini M, et al. Nanoparticles Engineering by Pulsed Laser Ablation in Liquids: Concepts and Applications. Nanomaterials. 2020;10(11):2317.
15. Huang H, Lai J, Lu J, Li Z. Pulsed laser ablation of bulk target and particle products in liquid for nanomaterial fabrication. AIP Advances. 2019;9(1).

CC BY